DOI: 10.1002/chem.200800077

A General Method for the Rapid Synthesis of Hollow Metallic or Bimetallic Nanoelectrocatalysts with Urchinlike Morphology

Shaojun Guo,[a, b] Shaojun Dong,*[a, b] and Erkang Wang[a, b]

Abstract: We have reported a facile and general method for the rapid synthesis of hollow nanostructures with urchinlike morphology. In-situ produced Ag nanoparticles can be used as sacrificial templates to rapidly synthesize diverse hollow urchinlike metallic or bimetallic (such as Au/Pt) nanostructures. It has been found that heating the solution at 100 °C during the galvanic replacement is very necessary for obtaining urchinlike nanostructures. Through changing the molar ratios of Ag to Pt, the wall thickness of hollow nanospheres can be easily controlled; through changing the diameter of Ag nanoparticles, the size of cavity of hollow nanospheres can be facilely controlled; through changing the morphologies of Ag nanostructures from nanoparticle to nanowire, hollow Pt nanotubes can be easily designed. This one-pot approach can be extended to synthesize other hollow nanospheres such as Pd, Pd/Pt, Au/Pd, and Au/Pt. The features of this technique are that it is facile, quick, economical, and versatile. Most importantly, the hollow bimetallic nanospheres (Au/Pt and Pd/Pt) obtained here exhibit an area of greater electrochemical activity than other Pt hollow or solid nanospheres. In addition, the ≈6 nm hollow urchinlike Pt nanospheres can achieve a potential of up to 0.57 V for oxygen reduction, which is about 200 mV more positive than that obtained by using a ≈6 nm Pt nanoparticle modified glassy carbon (GC) electrode. Rotating ring-disk electrode (RRDE) voltammetry demonstrates that ≈6 nm hollow Pt nanospheres can catalyze an almost four-electron reduction of O_2 to H_2O in air-saturated H_2SO_4 (0.5 M). Finally, compared to the ≈6 nm Pt nanoparticle catalyst, the ≈6 nm hollow urchinlike Pt nanosphere catalyst exhibits a superior electrocatalytic activity toward the methanol oxidation reaction at the same Pt loadings.

Keywords: fuel cells · methanol oxidation · nanostructures · platinum · silver

Introduction

In recent years, metal nanostructures with specific size and morphology have been strongly motivated by the requirements to uncover and map their size- and shape-dependent properties and to achieve their practical applications ranging from biomedicine to sensor, catalysis, optics, electronics, and optoelectronics.[1] In particular, hollow metal nanostructures have attracted more attention on account of their numerous potential applications in drug-delivery carriers, biomedical diagnosis agents, and cell imaging.[2–4] For example, the strong surface plasmon absorption of gold nanocages in the near-infrared region makes these nanomaterials ideal candidates for photothermally trigged drug release in tissues.[4] Hollow nanostructures can be obtained by using hard- and soft-template methods. Although the hard-template method[5–9] is an effective route for fabricating size-controlled hollow nanostructures, the preparation of the template is tedious and post-synthetic treatments are needed to remove them from the products, which might destroy as-prepared hollow nanospheres. Soft-template approaches including use of vesicles,[10–12] emulsions,[13–15] micelles,[16,17] and even gas bubbles[18] have been well developed by several groups, however, the addition of some surfactants may introduce contamination in the final product, owing to the formation of undesired byproducts in the reaction medium, which makes them unsuitable for further applications. Recently, the galvanic displacement reactions involving sacrificial metal nanoparticles and suitable metal ions provided a novel process for the synthesis of hollow nanostructured materials. For example, hollow Au,[19] Ag,[20] Pt,[21] and Au/Pt[22]

[a] S. Guo, Prof. S. Dong, Prof. E. Wang
State Key Laboratory of Electroanalytical Chemistry
Changchun Institute of Applied Chemistry
Chinese Academy of Sciences, Jilin 130022 (P.R. China)
E-mail: dongsj@ciac.jl.cn

[b] S. Guo, Prof. S. Dong, Prof. E. Wang
Graduate School of the Chinese Academy of Sciences
Changchun, Jilin 130022 (P.R. China)
Fax: (+86) 431-8568-9711

alloy nanostructures have been prepared by employing Co nanoparticles produced in-situ as a sacrificial template. However the process usually needs an inert atmosphere and can lead to a complex process when synthesizing Co nanoparticles. Furthermore, Xia et al.[4] reported that hollow nanostructures with smooth surfaces could be obtained by using Ag nanocubes as a sacrificial template. However, to further increase the efficient surface-to-volume ratios of hollow nanostructures in applications of nanocatalysis and nanobiosensors, it is still necessary to change hollow nanospheres to more a complex morphology such as our urchinlike nanostructure.

The search for abundant, inexpensive, and efficient electrocatalytic materials for oxygen reduction cathodes or methanol oxidation anodes in polymer electrolyte membrane fuel cells (PEMFC) is currently an active area of research. For numerous nanocatalysts, Pt and Pt-based nanomaterials are still indispensable and the most effective catalyst for fuel cells. However, a critical problem with Pt-based catalysts is their prohibitive cost. Therefore, it is very necessary to search for cost-effective routes to make more-efficient Pt catalysts. Recent efforts have focused on the development of novel techniques to prepare Pt-based catalysts with particular morphologies.[23–27] For example, Sun and coworkers[23] developed a simple high-temperature organic phase synthesis of monodisperse Pt nanocubes and studied their catalysis for oxygen reduction. Wang and coworkers[24] employed a facile electrochemical method for synthesizing unconventional tetrahexahedron Pt nanospheres with high-index surfaces for electrocatalytic applications. Although the maximization of high-index surfaces and abundant corner and edge sites should be the criteria for selection of an excellent nanocatalyst,[25] changing the solid Pt nanocatalyst to hollow nanostructures will greatly reduce the amount of Pt used and improve the efficient utility of Pt. Several groups have reported the synthesis of hollow Pt-based nanospheres for electrocatalytic applications,[21,22,28,29] but only hollow Pt nanospheres with smooth surfaces were employed as electrocatalysts. To further increase the surface-to-volume ratios of Pt, reducing the usage of expensive Pt and enhance the activity of Pt, it is necessary to change the Pt shell to a more complex morphology (e.g., an urchinlike nanostructure).

In this paper, a general method for the rapid synthesis of hollow nanostructures with specific morphology has been reported. It is found that the hollow urchinlike Pt nanostructures have been facilely obtained through a one-pot process. Such one-pot approach can be extended to synthesize other hollow nanospheres such Pd, Pd/Pt, Au/Pd, and Au/Pt. Furthermore, the applications of hollow Pt nanospheres with urchinlike structures in electrocatalytic dioxygen reduction and methanol oxidation were investigated. The higher peak currents associated with the hydrogen adsorption/desorption and oxide formation/reduction events provided by hollow Au/Pt or Pd/Pt nanospheres indicate that hollow Au/Pt or Pd/Pt nanospheres possess higher electroactive surface area than other hollow nanospheres (The Pt loadings are the same for all samples tested). It should be noted that the modified (with $\approx$6 nm hollow urchinlike Pt nanospheres) glassy carbon (GC) electrode exhibits much higher peak currents for dioxygen reduction and methanol oxidation than that of the Pt nanoparticles with similar sizes, indicating that the hollow Pt nanospheres with urchinlike morphology will greatly reduce the cost of the material.

Results and Discussion

The galvanic displacement reaction has been employed to synthesize hollow nanospheres with rough surfaces by using Co or Ag nanoparticles as sacrificial templates. Rapidly synthesizing hollow nanospheres with urchinlike surfaces, which is necessary for reducing the usage of expensive Pt, is still a great challenge.[30] Herein, the driving force of the galvanic replacement reaction comes from the reduction potential gap between the metallic precursor (such as $PtCl_6^{2-}$/Pt) and Ag^+/Ag redox couple. Most importantly, it is found that heating the solution at 100 °C during the galvanic replacement is very necessary for obtaining hollow urchinlike nanostructures. Figure 1A shows the typical TEM image of the

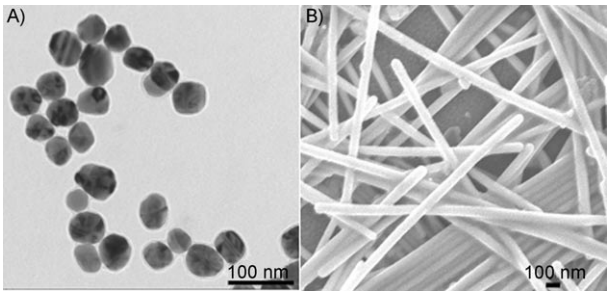

Figure 1. TEM images of A) big Ag nanoparticles and B) Ag nanowires.

as-prepared Ag nanoparticles before the galvanic replacement happens. A few of Ag nanoparticles with the diameter of about 50–60 nm are observed. As an example, $PtCl_6^{2-}$ ion was first employed for the galvanic replacement of Ag nanoparticles. Figure 2A,B show the typical SEM images of Pt nanospheres after galvanic replacement of Ag nanoparticles at different magnifications. It is observed that a great number of Pt nanospheres were obtained. To reveal the detailed structure, TEM was employed to characterize the obtained Pt nanospheres (Figure 2C,D). The strong contrast difference in all of the spheres, with a bright center surrounded by a much darker edge, confirms their hollow structure. The magnified image in Figure 2D shows a hollow Pt nanosphere with a wall thickness of $\approx$25 nm and an urchinlike structure. The wall thickness of hollow Pt nanospheres can be easily controlled by changing the molar ratio of Ag to metallic precursors. Addition of H_2PtCl_6 (1.25 mL, 1%) under the same conditions as those of the above sample, the wall thickness of hollow Pt nanospheres can be reduced to $\approx$15 nm (Figure 3A). Reduction of 1% H_2PtCl_6 to 0.5 mL, results in a wall thickness less than 10 nm (Figure 3B). The

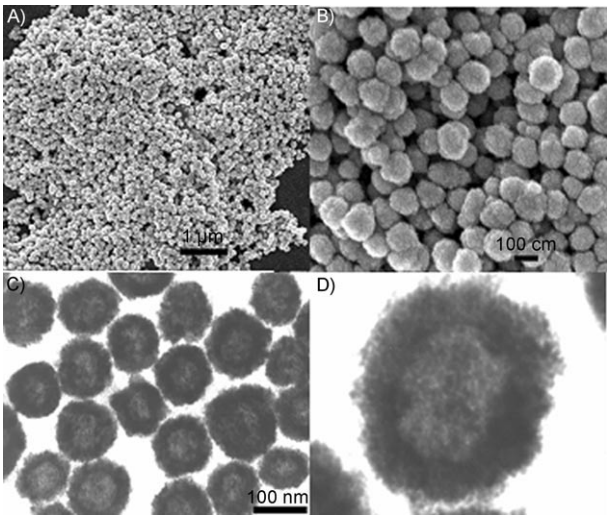

Figure 2. A,B) SEM and C,D) TEM images of big hollow urchinlike Pt nanospheres at different magnifications.

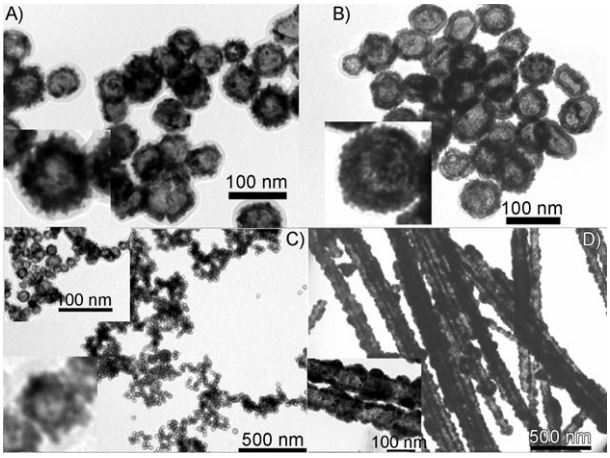

Figure 3. TEM images of big hollow urchinlike Pt nanospheres (A: 0.5 mL, B: 1.25 mL). TEM images of C) ≈6 nm hollow urchinlike Pt nanospheres and D) hollow Pt nanotubes.

size of the cavity of the hollow nanospheres can be facilely controlled by changing the diameter of as-synthesized Ag nanoparticles. Figure 3C shows the typical TEM image of ≈6 nm Pt nanospheres. From the magnified image, it can be seen that these nanospheres exist in the form of hollow urchinlike structures. If the Pt precursor is changed to Pd (Figure 4A), Pd/Pt (Figure 4B), Au/Pd (Figure 4C) or Au/Pt (Figure 4D), hollow urchinlike nanospheres can also be easily obtained. Furthermore, through changing the morphologies of Ag nanostructures from nanoparticles to nanowires, hollow Pt nanotubes with rough surfaces can be easily designed. Figure 1B shows the typical TEM image of the as-prepared Ag nanowires. The diameter of these nanowires is about 80–90 nm. After reacting with Pt precursor, hollow Pt nanotubes with rough surfaces can be easily synthesized (Figure 3D).

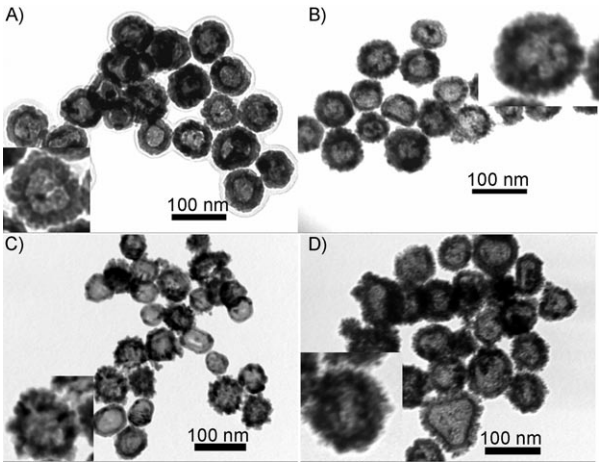

Figure 4. A) TEM images of hollow Pd nanospheres, B) hollow Pd/Pt (1:1) nanospheres, C) hollow Au/Pd (1:1) nanospheres, and D) hollow Au/Pt (1:1) nanospheres.

X-ray photoelectron spectroscopy (XPS) was further employed to investigate the composition of hollow Pt nanospheres. XPS pattern of the hollow Pt nanospheres shows significant Pt-4f signal, corresponding to the binding energy of metallic Pt (Figure 5A), that indicates that Pt precursor

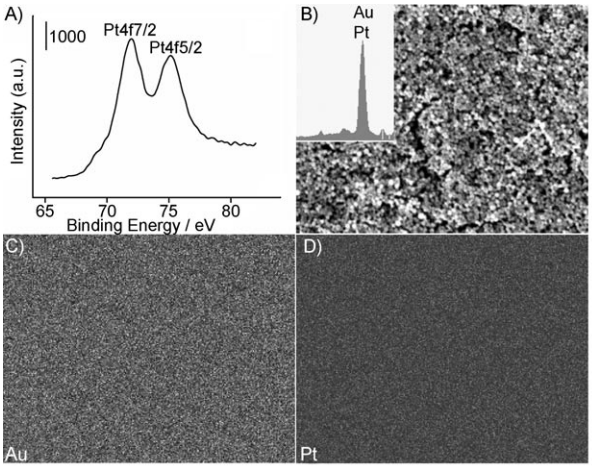

Figure 5. A) XPS spectrum of the as-prepared ≈6 nm hollow urchinlike Pt nanospheres; B–D) X-ray maps of hollow Au/Pt spheres. The inset of B) shows the EDS image of hollow Au/Pt spheres.

has been reduced to metallic Pt. Notably, the introduction of a strong reducing reagent such as $NaBH_4$ to the as-formed hollow Pt nanosphere does not result in further change of the solution color. This would suggest that the additional Pt salts have been totally reduced by ascorbic acid during the thermal process. The chemical composition of the Au/Pt hollow bimetallic nanosphere was determined by energy-dispersed spectrum (EDS, the inset of Figure 5B) and X-ray maps analysis of the products coated on silicon slide (Figure 5B–D). The EDS spectrum (the inset of Fig-

ure 5B) shows peaks corresponding to Au and Pt elements (the other peaks originate from the substrate). The corresponding X-ray maps (Figure 5C,D) reveal that the elements Au and Pt are relatively uniformly distributed throughout these nanospheres. Based on these observations, we can conclude that Au/Pt bimetallic nanospheres can be indeed obtained. Similar analysis of hollow Au/Pd nanospheres, the same conclusion can be obtained (data not shown).

Figure 6 shows cyclic voltammograms (CVs) of hollow big urchinlike Pt spheres with different wall thickness (a, b, and c), ≈6 nm hollow urchinlike Pt sphere (d), Au/Pt hollow

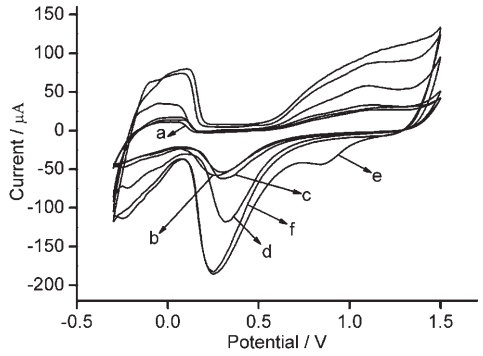

Figure 6. Cyclic voltammograms of big hollow Pt nanospheres (a: 0.5 mL), big hollow Pt nanospheres (b: 1.25 mL), big hollow Pt nanospheres (c: 2.5 mL), ≈6 nm hollow Pt nanoparticle (d), hollow Au/Pt nanospheres (e), and hollow Pd/Pt nanospheres (f) modified GC electrode in a N_2 sparged H_2SO_4 (0.5 M) solution at scan rate of 50 mV s^{-1}.

sphere (e) and hollow Pd/Pt sphere catalysts (f) in H_2SO_4 (0.5 M) acquired at a scan rate of 50 mV s^{-1}. A comparison of hydrogen adsorption/desorption and metal oxidation/reduction events of these catalysts indicates that the active electrochemical area of the larger urchinlike hollow Pt spheres with different sizes is similar under the conditions of same Pt loadings. However, if the diameter of the Ag nanoparticles is reduced to ≈3 nm, the obtained ≈6 nm hollow Pt nanospheres exhibit an area of greater electrochemical activity than the above larger hollow Pt nanospheres. Notably, the larger hollow Au/Pt or Pd/Pt bimetallic nanospheres have greater electrochemical active areas than the ≈6 nm hollow Pt nanospheres, probably a result of the efficiency of the alloy in the nanostructure.[31] The Pt utilization decreases in the order of Au/Pt, Pd/Pt > 6 nm hollow Pt spheres > hollow Pt spheres with different wall thickness. As a reference, ≈6 nm Pt nanoparticles were also investigated by cyclic voltammetry (at a scan rate of 50 mV s^{-1}) in H_2SO_4 (0.5 M). The current densities in the hydrogen adsorption/desorption and oxide formation/reduction regions of the ≈6 nm hollow urchinlike Pt spheres (Figure 7b) are much larger than that of ≈6 nm Pt nanoparticles (Figure 7a), indicating a larger area of electrochemical activity for hollow Pt nanospheres, which are believed to be a result of the hollow urchinlike structure. In addition, in the oxide formation/reduction regions of the Au/Pt hollow nanospheres (Fig-

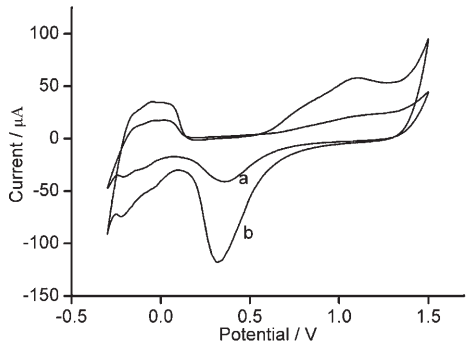

Figure 7. Cyclic voltammograms of ≈6 nm hollow Pt nanosphere (b) and ≈6 nm Pt nanoparticle (a) modified GC electrode in a N_2 sparged H_2SO_4 (0.5 M) solution at scan rate of 50 mV s^{-1}.

ure 6e), an obvious reduction peak of gold oxide is located at ≈0.8 V, which also suggests that the as-prepared hollow nanospheres are bimetallic.

The oxygen reduction reaction (ORR) is a reaction of indispensable importance in metal–air batteries and fuel cells as well as in oxygen sensors. The electroreduction of dioxygen usually requires high current density, low overpotential, and nearly synchronous delivery of four electrons. Figure 8d

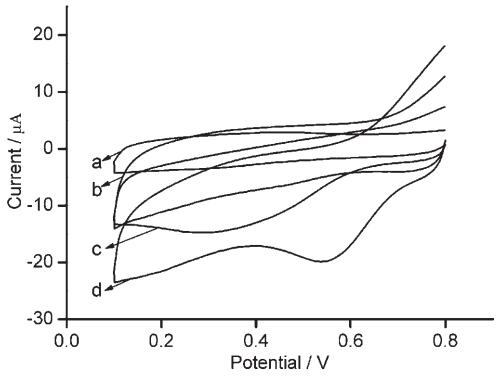

Figure 8. Cyclic voltammograms of O_2 reduction at the ≈6 nm hollow Pt nanosphere (b and d), ≈6 nm Pt nanoparticle (c) modified GC electrode, bare GC electrode (a) in air-saturated (a, c, d) and N_2-saturated (b) H_2SO_4 (0.5 M) solution. Scan rate: 50 mV s^{-1}.

shows the typical CV of dioxygen reduction at the modified (with ≈6 nm hollow Pt nanospheres) GC electrode in a H_2SO_4 (0.5 M) solution in the presence of air. A remarkable catalytic reduction current occurs at 0.57 V at a scan rate of 50 mV s^{-1}. No catalytic reduction current can be observed in the presence of N_2 (Figure 8b), this indicates that the catalytic current located at 0.57 V can be ascribed to the reduction of oxygen. As a comparison, Figure 8a shows the CV of dioxygen reduction at the bare GC electrode in the presence of air. No catalytic reduction current can be observed. To further reveal high electrocatalytic performance of ≈6 nm hollow urchinlike Pt nanospheres, the ORR of Pt nanoparticles of comparable size has also been investigated. Figure 8c show that typical CV of dioxygen reduction at the ≈6 nm Pt

nanoparticles modified GC electrode in a H_2SO_4 (0.5 M) solution in the presence of air. It is found that ≈6 nm hollow urchinlike Pt nanosphere modified GC electrode (Figure 8d) exhibits more positive potential and higher current for dioxygen reduction than that obtained from ≈6 nm Pt nanoparticles (Figure 8c), indicating that the present hollow urchinlike Pt nanosphere modified GC electrode shows higher electrocatalytic activity than that of the ≈6 nm Pt nanoparticles.

We have shown that ≈6 nm urchinlike Pt hollow nanospheres exhibit a high catalytic current and a low overpotential for the reduction of oxygen. The additional important index is the four-electron electroreduction of dioxygen to water, which is a reaction greatly pursued by scientists in view of its important application in fuel cells. Consequently, the ORR was probed through a rotating ring-disk electrode (RRDE) experiment to demonstrate the ORR process of ≈6 nm hollow urchinlike Pt nanosphere modified electrode. The as-prepared ≈6 nm Pt hollow sphere modified GC electrode reduces O_2 by almost four electrons to H_2O, as confirmed by the RRDE technique. Figure 9 shows the voltammetric curves for dioxygen reduction, recorded at the RRDE with the ≈6 nm hollow Pt nanosphere immobilized on the GC disk electrode. In this experiment, disk potential was scanned from +0.85 to 0.15 V, while the ring potential was kept at +1.0 V order to detect any H_2O_2 evolved at the disk. A large disk current was obtained, whereas almost no ring current was observed, which suggests that the as-prepared hollow nanostructured electrocatalysts reduce O_2 by almost four electrons to H_2O. From the ratio of the ring-disk current, the electron-transfer number (n) is calculated to be ≈4 according to the equation $n = 4–2(I_R/I_D N)$.[32]

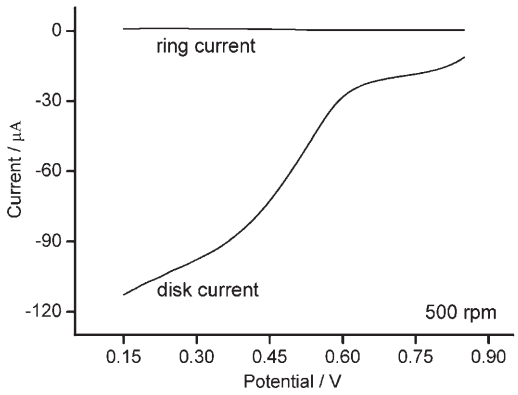

Figure 9. Current–potential curves for the reduction of H_2O in the air-saturated electrolyte H_2SO_4 (0.5 M) at a rotating platinum ring-GC electrode with ≈6 nm hollow Pt nanospheres adsorbed on the disk electrode. The potential of the ring electrode was maintained at 1.0 V. Rotation rate: 500 rpm; Scan rate: 50 mV s^{-1}.

Another important electrocatalytic reaction, which is deeply studied by scientists, is methanol electrocatalytic oxidation. Herein, the electrocatalytic activity of the hollow urchinlike Pt spheres toward the oxidation of methanol was also tested and the results were compared with those obtained from ≈6 nm Pt nanoparticles. The measurements were carried out in a H_2SO_4 (0.5 M) aqueous solution containing methanol (1.0 M). A GC electrode with a diameter of about 4 mm was used as the working electrode. Figure 10 shows the voltammetry curves of ≈6 nm hollow urchinlike Pt nanospheres (c) and ≈6 nm Pt nanoparticles (b) modified GC electrodes in H_2SO_4 (0.5 M) containing 1 M methanol. It is found that the hollow Pt nanosphere modified GC electrode shows catalytic behavior for the electrooxidation of methanol by the appearance of an oxidation current in the positive potential region. The onset potentials are around 0.25 V (vs. Ag/AgCl). The peak current at about 0.75 V (vs. Ag/AgCl) in the forward scan is attributed to methanol electrooxidation at the hollow Pt nanosphere. In the reverse scan, an oxidation peak is observed around 0.50 V, which is probably associated with the removal of the residual carbon species formed in the forward scan.[30] Although two samples show catalytic activities toward the methanol oxidation, the peak currents catalyzed by the hollow urchinlike Pt sphere are about 2 times larger than that of the ≈6 nm Pt nanoparticles (The Pt loadings for two sample tested are the same, 3.76 μg). The important reason for the high catalytic property could be attributed to the fact that the ≈6 nm Pt nanospheres presented here have hollow urchinlike nanostructures. As a comparison, methanol electrocatalytic oxidation was also investigated on bare GC electrode (Figure 10a). No oxidation peaks of methanol are observed, indicating that electrocatalytic current observed in Figure 10c can probably be ascribed to high electrocatalytic activity of the hollow Pt nanosphere with high surface-to-volume ratios. Although we just compare the electrocatalytic activity of ≈6 nm hollow Pt spheres with ≈6 nm Pt nanoparticles, it is expected that hollow Au/Pt or Pd/Pt bimetallic nanospheres with urchinlike structure will have higher electrocatalytic activity than ≈6 nm hollow Pt nanospheres under the same Pt loadings. This is because the modified (with Au/Pt or Pd/Pt bimetallic

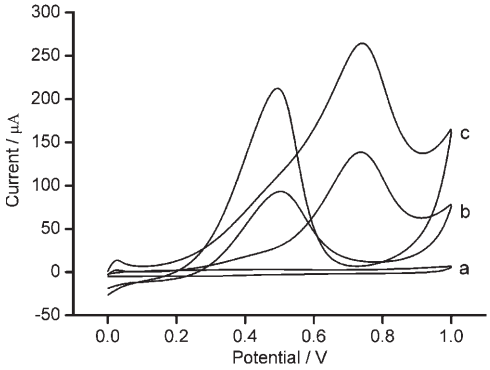

Figure 10. Cyclic voltammograms of methanol oxidation at the ≈6 nm hollow Pt nanospheres (c), ≈6 nm Pt nanoparticles (b) modified GC electrode, bare GC electrode (a) in H_2SO_4 (0.5 M) solution containing methanol (1 M). Scan rate: 50 mV s^{-1}.

hollow nanospheres) GC electrode has an area of greater electrochemical activity than other Pt based nanostructures.

Considering the particular structure of ≈6 nm Pt hollow spheres, two important factors should be responsible for the above high electrocatalytic activity. First, the 6 nm hollow Pt nanospheres have urchinlike structures. These urchinlike structures (Figure 1) have a rough surface, which will increase the efficiency of the active area of Pt. Second, the size of hollow Pt nanospheres is less than 10 nm, which has been reported to be of vital importance to high electrocatalytic performance.[32] Most importantly, Pt nanospheres existing in the form of hollow structures will greatly reduce the dosage of expensive Pt, which is important for the development of fuel cells.

Conclusion

By taking advantage of the recent advances in nanotechnology, we have reported a facile and general method for rapid synthesis of hollow metallic or bimetallic nanostructures with specific morphology. This one-pot approach can be extended to synthesize other hollow nanospheres such Pd, Pd/Pt, Au/Pd, and Au/Pt. Furthermore, the electrocatalytic applications of the obtained hollow spheres with rough surfaces were investigated. It was found that the Au/Pt or Pd/Pt hollow nanospheres exhibit an area of greater electrochemical activity than other Pt-based nanospheres. The potential for oxygen reduction on ≈6 nm hollow Pt nanospheres reaches up to 0.57 V, which is about 200 mV higher than that obtained from the ≈6 nm Pt nanoparticle modified GC electrode. RRDE voltammetry further demonstrates that ≈6 nm hollow urchinlike Pt nanospheres can catalyze the four-electron reduction of O_2 to H_2O in air-saturated H_2SO_4 (0.5 M). Thus, these hollow urchinlike nanospheres well meet the three important criterions needed by ORR of fuel cells. Finally, compared to the ≈6 nm Pt nanoparticle catalyst, the ≈6 nm hollow urchinlike Pt nanosphere catalyst exhibits a higher electrocatalytic activity toward the methanol oxidation reaction at the same Pt loading.

Experimental Section

Chemicals: Tri-sodium citrate, ethylene glycol (EG), poly(vinyl pyrrolidone) (PVP·K30), vitamin C (VC), $AgNO_3$, $HAuCl_4{\cdot}4H_2O$, $H_2PtCl_6{\cdot}6H_2O$ and H_2SO_4 were purchased from Beijing Chemical Factory (Beijing, China) and used as received without further purification. $PdCl_2$, $NaBH_4$, and Nafion (perfluorinated ion-exchange resin, 5 wt% solution in a mixture of lower aliphatic alcohols and water) were purchased from Aldrich and used as received. Water used throughout all these experiments was purified with a Millipore system.

Apparatus: A XL30 ESEM scanning electron microscope equipped with an energy-dispersive X-ray analyzer was used to determine the morphology and composition of products. Transmission electron microscopy (TEM) was carried out by using a HITACHI H-8100 EM with an accelerating voltage of 200 kV. The sample for TEM characterization was prepared by placing a drop of sample solution on a carbon-coated copper grid and dried at room temperature. X-ray photoelectron spectroscopy (XPS) measurements were performed by using ESCALAB-MKII spectrometer (VG Co., United Kingdom) with $Al_{K\alpha}$ X-ray radiation as the source for excitation. The sample for XPS characterization was deposited on a glass plate. Cyclic voltammetric experiments were performed by using a CHI 832 electrochemical analyzer (CH Instruments, Chenhua Co., Shanghai, China). A conventional three-electrode cell was used, including a Ag/AgCl (saturated KCl) reference electrode, a platinum wire as the counter electrode and a bare or modified GC (4 mm) as the working electrode. An EG&G PARC Model 366 bi-potentiostat was used for RRDE experiments. A rotating GC (5 mm) disk-platinum ring electrode was used as a working-electrode. The collection efficiency (N) of the ring electrode obtained by reducing ferricyanide at a disk electrode was 0.139.

Synthesis of Ag nanoparticles: All glassware used in the following procedures were cleaned in a bath of freshly prepared 3:1 HCl: HNO_3 (aqua regia) and rinsed thoroughly in milli-Q grade water prior to use. In a typical synthesis of Ag nanoparticles with the diameter of 50–60 nm, 0.125 mL of $AgNO_3$ (0.2 M) aqueous solution was rapidly added into 50 mL water accompanied by vigorous stirring. After heating to boil, citrate (3 mL, 1%) aqueous solution was quickly added to the above solution, and followed by adding VC (2 mL, 0.1 M). A quick color change from yellow to grey-yellow was observed upon the addition of VC. After heating for 5 min, the solution was stored under ambient conditions for characterization. For the synthesis of Ag nanoparticles with a diameter of ≈3 nm, the same procedure as above was employed except $NaBH_4$ (1 mL, 0.1 M) was added at the final step. Note that the as-prepared ≈3 nm Ag nanoparticles were stored under ambient conditions before further experiments.

Synthesis of Pt nanoparticles (≈6 nm): The Pt nanoparticles with the diameter of ≈6 nm were synthesized according to the literature.[32] Briefly, one milliliter of H_2PtCl_6 (1%) aqueous solution was added to water (100 mL) and then heated to boiling. To this sodium citrate (3 mL, 1%) aqueous solution was added rapidly, and the mixture was kept at a boiling temperature for ≈30 min.

Synthesis of Ag nanowires: Silver nanowires were synthesized according to the method reported by Yan et al.[33] In a typical synthesis, EG (50 mL) was heated in a three-necked round-bottom flask (equipped with a condenser, thermocontroller, and magnetic stirring bar) at 165 °C for 1 h. Subsequently, H_2PtCl_6 solution (5 mL, 0.2 mM in EG) was added. After 5 min, $AgNO_3$ solution (25 mL, 0.12 M in EG) and PVP solution (50 mL, 0.36 M in EG) were added dropwise (simultaneously) to the hot solution over 6 min, and the reaction continued at 165 °C for 50 min. Vigorous stirring was maintained throughout the entire process. To purify the product, the reaction mixture was diluted with water and centrifuged at 8000 rpm for 10 min.

Preparation of hollow nanostructures with urchinlike morphology: In a typical synthesis, $AgNO_3$ (0.125 mL, 0.2 M) aqueous solution was rapidly added to water (50 mL) accompanied by vigorous stirring. After heating to the boil, citrate (3 mL, 1%) aqueous solution was quickly added to the above solution, and followed by the addition of VC (2 mL, 0.1 M). A quick color change from yellow to grey-yellow was observed upon the addition of VC. After heating for 5 min, H_2PtCl_6 (2.5 mL, 1%) aqueous solution was dropwise added to the above heating solution and followed by heating for about 20 min. Subsequently, the reaction solution was centrifuged at 8000 rpm three times and dissolved in 25 mL water.

Electrocatalytic experiment: The electrode was loaded with hollow nanostructures or Pt nanoparticles (10 μL, the same Pt loadings of 3.76 μg for samples tested). Electrocatalytic dioxygen reduction measurements were carried out in a H_2SO_4 (0.5 M) solution in the presence of air or N_2 at the scan rate of 50 mV s^{-1}. For the RRDE voltammetry experiments, ≈6 nm Pt hollow nanosphere solution (20 μL) was deposited on the GC electrode (5 mm) and allowed to dry at room temperature. Nafion (5 μL, 0.2%) was placed on the surface of the Pt hollow sphere modified GC electrode. The RRDE experiment was performed in air-saturated H_2SO_4 (0.5 M), and disk potential was scanned from +0.85 to 0.15 V while the ring potential was kept at +1.0 V in order to detect any H_2O_2 evolved at the disk.

Acknowledgements

This work was supported by the National Science Foundation of China (Nos. 20575064, 20675076 and 20427003).

[1] M. Daniel, D. Astruc, *Chem. Rev.* **2004**, *104*, 293.
[2] E. Mathiowitz, J. S. Jacob, Y. S. Jon, G. P. Carino, D. E. Chickering, P. Chaturvedi, C. A. Santos, K. Vijayaraghavan, S. Montgomery, M. Bassett, C. Morrell, *Nature* **1997**, *386*, 410.
[3] J. Chen, F. Saeki, B. Wiley, H. Cang, M. J. Cobb, Z. Li, L. Au, H. Zhang, M. J. Kimmey, X. Li, Y. Xia, *Nano Lett.* **2005**, *5*, 473.
[4] J. Chen, D. Wang, J. Xi, L. Au, A. Siekkinen, A. Warsen, Z.-Y. Li, H. Zhang, Y. Xia, X. Li, *Nano Lett.* **2007**, *7*, 1318.
[5] V. Salgueirino-Maceira, M. Spasova, M. Farle, *Adv. Funct. Mater.* **2005**, *15*, 1036.
[6] F. Caruso, M. Spasova, V. Saigueirino-Maceira, L. M. Liz-Marzan, *Adv. Mater.* **2001**, *13*, 1090.
[7] Z. Yang, Z. Niu, Y. Lu, Z. Hu, Han, C. C. *Angew.Chem. Int. Ed.* **2003**, *42*, 1943.
[8] Z. Yang, Z. Niu, Y. Lu, Z. Hu, C. C. Han, *Angew. Chem.* **2003**, *115*, 4333; *Angew. Chem. Int. Ed.* **2003**, *42*, 4201.
[9] Y. D. Xia, R. Mokaya, *J. Mater. Chem.* **2005**, *15*, 3126.
[10] H. T. Schmidt, A. E. Ostafin, *Adv. Mater.* **2002**, *14*, 532.
[11] D. H. W. Hubert, M. Jung, A. L. German, *Adv. Mater.* **2000**, *12*, 1291.
[12] H. P. Hentze, S. R. Raghavan, C. A. McKelvey, E. W. Kaler, *Langmuir* **2003**, *19*, 1069.
[13] T. Hirai, S. Hariguchi, I. Komasawa, R. J. Davey, *Langmuir* **1997**, *13*, 6650.
[14] M. M. Wu, G. G. Wang, H. F. Xu, J. B. Long, F. L. Y. Shek, S. M. F. Lo, I. D. Williams, S. H. Feng, R. R. Xu, *Langmuir* **2003**, *19*, 1362.
[15] C. E. Fowler, D. Khushalani, S. Mann, *Chem. Commun.* **2001**, 2028.
[16] C. E. Fowler, D. Khushalani, S. Mann, *J. Mater. Chem.* **2001**, *11*, 1968.
[17] J. X. Huang, Y. Xie, B. Li, Y. Liu, Y. T. Qian, S. Y. Zhang, *Adv. Mater.* **2000**, *12*, 808.
[18] F. L. Du, Z. Y. Guo, G. C. Li, *Mater. Lett.* **2005**, *59*, 2563.
[19] H. P. Liang, L. J. Wan, C. L. Bai, L. Jiang, *J. Phys. Chem. B* **2005**, *109*, 7795.
[20] M. H. Chen, L. Gao, *Inorg. Chem.* **2006**, *45*, 5145.
[21] H. P. Liang, H. M. Zhang, J. S. Hu, Y. G. Guo, L. J. Wan, C. L. Bai, *Angew. Chem.* **2004**, *116*, 1566; *Angew. Chem. Int. Ed.* **2004**, *43*, 1540.
[22] H. Liang, Y. Guo, H. Zhang, J. Hu, L. Wan, C. Bai, *Chem. Commun.* **2004**, 1496.
[23] C. Wang, H. Daimon, Y. Lee, J. Kim, S. Sun, *J. Am. Chem. Soc.* **2007**, *129*, 6974.
[24] N. Tian, Z. Y. Zhou, S. G. Sun, Y. Ding, Z. L. Wang, *Science* **2007**, *316*, 732.
[25] Y. Xiong, B. J. Wiley, Y. Xia, *Angew. Chem.* **2007**, *119*, 7291; *Angew. Chem. Int. Ed.* **2007**, *46*, 7157.
[26] S. Maksimuk, S. Yang, Z. Peng, H. Yang, *J. Am. Chem. Soc.* **2007**, *129*, 8684.
[27] M. Chen, T. Pica, Y. Jiang, P. Li, K. Yano, J. P. Liu, A. K. Datye, H. Fan, *J. Am. Chem. Soc.* **2007**, *129*, 6348.
[28] B. Mayers, X. Jiang, D. Sunderland, B. Cattle, Y. Xia, *J. Am. Chem. Soc.* **2003**, *125*, 13364.
[29] G. Chen, D. Xia, Z. Nie, Z. Wang, L. Wang, L. Zhang, J. Zhang, *Chem. Mater.* **2007**, *19*, 1840.
[30] S. Guo, Y. Fang, S. Dong, E. Wang, *J. Phys. Chem. C* **2007**, *111*, 17104.
[31] J. L. Fernández, D. A. Walsh, A. J. Bard, *J. Am. Chem. Soc.* **2005**, *127*, 357.
[32] M. Huang, Y. Jin, H. Jiang, X. Sun, H. Chen, B. Liu, E. Wang, S. Dong, *J. Phys. Chem. B* **2005**, *109*, 15264.
[33] Z. Chen, M. Waje, W. Li, Y. Yan, *Angew. Chem.* **2007**, *119*, 4138; *Angew. Chem. Int. Ed.* **2007**, *46*, 4060.

Received: January 14, 2008
Published online: April 2, 2008

